Published in final edited form as:
J Immunol. 2014 October 15; 193(8): 3914–3924. doi:10.4049/jimmunol.1303116.

CD47 signaling regulates the immunosuppressive activity of VEGF in T cells*

Sukhbir Kaur[†], **Tiffany Chang**[†], **Satya P. Singh**[‡], **Langston Lim**[§], **Poonam Mannan**[§], **Susan H. Garfield**[§], **Michael L. Pendrak**[†], **David R. Soto Pantoja**[†], **Avi Z. Rosenberg**[†], **Shelly Jin**[†], and **David D. Roberts**[†,¶]

[†]Laboratory of Pathology, Center for Cancer Research, National Cancer Institute, National Institutes of Health, Bethesda MD 20982-1500

[‡]Laboratory of Molecular Immunology, National Institute of Allergy and Infectious Diseases, National Institutes of Health, Bethesda MD 20982-1886

[§]Laboratory of Experimental Carcinogenesis, Center for Cancer Research, National Cancer Institute, National Institutes of Health, Bethesda MD 20892-4262

Abstract

Thromobospondin-1 inhibits angiogenesis in part by interacting with the ubiquitous cell surface receptor CD47. In endothelial cells, CD47 interacts directly with vascular endothelial growth factor receptor-2 (VEGFR2), and thrombospondin-1 inhibits VEGFR2 phosphorylation and signaling by disrupting this association. We now show that CD47 similarly associates with and regulates VEGFR2 in T cells. Thrombospondin-1 inhibits phosphorylation of VEGFR2 and its downstream target Src in wild type but not in CD47-deficient human Jurkat and primary murine T cells. VEGFR2 signaling inhibits proliferation and TCR signaling in wild type T cells. However, ligation of CD47 by thrombospondin-1 or loss of CD47 expression reverses some inhibitory effects of VEGF on proliferation and T cell activation. We further found that VEGF and VEGFR2 expression are up-regulated in CD47-deficient murine $CD4^+$ and human Jurkat T cells, and the resulting autocrine VEGFR2 signaling enhances proliferation and some TCR responses in the absence of CD47. Thus, CD47 signaling modulates the ability of VEGF to regulate proliferation and TCR signaling, and autocrine production of VEGF by T cells contributes to this regulation. This provides a mechanism to understand the context-dependent effects of thrombospondin-1 and VEGF on T cell activation and reveals an important role for CD47 signaling in regulating T cell production of the major angiogenic factor VEGF.

Introduction

Vascular endothelial growth factor-A (VEGF) is a critical growth factor for endothelial cells, and even a moderate decrease in VEGF gene dosage is lethal for embryonic vascular development (1). Conversely, many cancer patients have elevated levels of circulating

*This work was supported by the NIH Intramural Research Programs of the NCI (D.D.R., S.H.G.).

¶Correspondence: NIH, Building 10 Room 2A33, 10 Center Drive, Bethesda, MD 20892-1500 Tel: 301-594-5256; droberts@helix.nih.gov.

VEGF, and VEGF is a major driver of tumor neovascularization (2). In addition to stimulating angiogenesis, some tumor cells express the VEGF tyrosine kinase receptors VEGFR1 and VEGFR2, and VEGF can be an autocrine growth and motility factor for these cancers (3-8). Based on these functions in tumor growth, several drugs targeting VEGF or the kinase activity of VEGFR2 have proven effective for controlling tumor angiogenesis and growth (9). However, many cancers develop resistance to VEGF antagonists, and tumor vascular responses to treatment may not correlate with improved survival (10).

The immune system is emerging as another important target of VEGF (11, 12). High levels of VEGF result in immunosuppression by inhibiting dendritic cell functions (13-17). Human $CD4^+CD45RO^+$ T cells and Jurkat T lymphoma cells express VEGFR1 and VEGFR2 at the mRNA and protein levels (18). Expression of VEGF and its receptors VEGFR1 and VEGFR2 is induced in T lymphocytes activated by anti-CD3 and anti-CD28 (19, 20). VEGF induces AKT and ERK phosphorylation in T cells, which can be inhibited by VEGFR2-siRNA. VEGF signaling via VEGFR2 inhibits proliferation of T lymphocytes derived from ovarian cancer patients and normal volunteers (19). Despite some inconsistencies, these reports demonstrate that VEGF and its receptors are expressed and functional in T cells, and therapeutic VEGF antagonists may consequently have effects on tumor immunity that could be exploited to improve their efficacy.

Further insights into this process may come from studies of endogenous antagonists of VEGF signaling such as thrombospondin-1 (TSP1). TSP1 inhibits tumor angiogenesis and blocks endothelial cell proliferation and chemotaxis by engaging its receptors CD36 and CD47 (21). Binding of the C-terminal domain of TSP1 to CD47 (also known as integrin-associated protein) redundantly inhibits eNOS/NO/cGMP signaling in endothelial cells (22). We recently demonstrated that TSP1 signaling through CD47 also inhibits VEGFR2 phosphorylation at Y^{1175} in human umbilical vein and dermal microvascular endothelial cells (23). However, TSP1 is unable to inhibit VEGFR2 phosphorylation in CD47-null endothelial cells. TSP1 signaling via CD47 suppresses VEGF induced VEGFR2 phosphorylation without inhibiting VEGF binding. Based on FRET data and co-immunoprecipitation, CD47 laterally associates with VEGFR2 in the absence of their respective ligands. TSP1 binding to CD47 dissociates it from VEGFR2, inhibiting downstream AKT activation and functional responses of endothelial cells to VEGF.

Initial reports that certain immobilized CD47 antibodies enhance T cell activation suggested that CD47 is a costimulatory receptor (24, 25). However, microarray data and signal transduction studies revealed that TSP1 globally inhibits TCR signaling induced by anti-CD3 (26), and this inhibitory activity requires CD47 (27-29). A prolonged T cell inflammatory response in CD47 and TSP1 null mice and *in vitro* studies using human T cells further indicate that TSP1 signaling through CD47 directly and indirectly limits T cell activation (30, 31).

The findings that VEGF and TSP1 signaling via CD47 separately inhibit TCR-mediated T cell activation combined with our recent identification of the TSP1 receptor CD47 as a VEGFR2 regulator in endothelial cells suggested that CD47 may also modulate the immunoinhibitory activity of VEGF. However, the outcome of this interaction was difficult

to predict given that TSP1 and VEGF elicit opposing signals through the CD47/VEGFR2 complex in endothelial cells. We now demonstrate that ligation of CD47 by TSP1 inhibits VEGFR2 signaling in T cells in a similar manner as in endothelial cells. VEGF signaling through VEGFR2 inhibits TCR-dependent activation in Jurkat and primary murine T cells but, remarkably, not in human or mouse T cells lacking CD47. Conversely, CD47 signaling regulates the expression of VEGF and VEGF receptors by T cells, and we show that CD47 signaling determines whether VEGF is an autocrine inhibitor or enhancer of T cell activation.

Materials and Methods

Cell culture and reagents

Jurkat T lymphoma cells (ATCC) and CD47-deficient JinB8 Jurkat cells (32) were cultured at 37°C with 5% CO_2 in RPMI1640 medium. WT and CD47 null C57Bl/6J mice (The Jackson Laboratory) were housed in a specific pathogen-free environment and had ad libitum access to standard rat chow and water. Care and handling of animals and all experimental procedures used here were approved under protocol LP-012 and in compliance with standards established by the Animal Care and Use Committee of the National Cancer Institute. Pan anti-$CD3^+$, $CD4^+$, $CD8^+$, $CD11b^+$ and $CD19^+$ cell isolation kits were used to isolate T cells from mouse WT and $CD47^{-/-}$ null spleens according to the manufacturer's instructions (Miltenyi Biotech, USA).

The TSP1-derived CD47-binding peptide 7N3 (FIRVVMYEGKK) and inactive control peptide 604 (FIRGGMYEGKK) were synthesized by Peptides International (Louisville) (33). Human TSP1 was purified from the supernatant of thrombin-activated platelets obtained from the NIH Blood Bank as described (34). VEGF-165 was obtained from R&D Biosystems (Minneapolis, MN, USA) or generously provided by Frank Cuttitta (ATC, NCI). Alexa Fluor 594 donkey anti-rabbit IgG and Alexa Fluor488 goat anti-mouse IgG antibodies were purchased from Invitrogen (MD, USA). VEGFR2, Y^{1175}-P, Src, and Src Y^{416}-P antibodies were obtained from Cell Signaling (Danvers, MA, USA). Anti-CD69 was obtained from BD biosciences. Anti-human CD47 antibody B6H12 was obtained from Abcam, biotinylated anti-human CD47 antibody was from Biolegend, and CD47-FITC was from BD Biosciences. Human VEGFR Phycoerythrin MAb Sampler (R&D Systems) containing PE-conjugated anti-VEGFR1 (clone 49560), VEGFR2 (clone 89106), and VEGFR3 (clone 54733) was used for flow cytometry. VEGF blocking antibody was from Sigma.

The Y^{1175}F mutation in the VEGFR2-mCherry fusion vector Ex-I0114-M56 (GeneCopoeia) was generated using PCR primer 5'-AGCAGGATGGCAAAGAC<u>TTC</u>ATTGTTCTTCCGATATC-3' and its reverse complement with the Quickchange Lightning kit (Stratagene Agilent Technologies). Using the protocol supplied by the manufacturer. This modified nucleotides 3523-3525 from TAC to TTC (underlined) to generate the Y^{1175}F codon change in the VEGFR2 coding sequence.

Transfection

The VEGFR2-mCherry fusion vector Ex-I0114-M56 and CD47-GFP (Dr. Dennis E. Discher) plasmid DNA either together or alone were transfected into Jurkat and JinB8 T cells using FuGENE® HD Transfection Reagent (Promega, Madison WI). At 24 h post-transfection, the GFP and mCHERRY positive cells were sorted via flow and used for FRET experiments.

Similarly, Jurkat T cells were transfected with VEGFR2-mCherry (WT) and VEGFR2–mCherry (mutant) plasmid DNA using FuGENE® HD Transfection Reagent. The Jurkat T cells were labeled using CellTrace™ CFSE Cell Proliferation Kit-for Flow Cytometry according to the manufacturer's instructions.

Endogenous Immunofluorescence

Jurkat WT and JinB8 T cells were grown overnight and serum starved for 2 h in RPMI 1640 basal medium containing 0.1% BSA. Jurkat T cells were plated in Labtek II chambers (Rochester) coated with poly D-lysine. The cells were washed gently three times with cold PBS. The cells were fixed with 4% paraformaldehyde for 15 min at RT and washed with PBS three times for 5 min intervals. Cells were permeabilized with 0.1% Triton X100 for 2 min and washed immediately with PBS 5 minutes each. Cells were blocked with 1% BSA in PBS-0.1% Tween 20 for 1h at RT. The cells were incubated in the mixture of two primary antibodies (1:300) mouse anti human CD47 (B6H12) and rabbit against anti-human VEGFR2 (1:500) (Cell Signaling) overnight at 4°C. The cells were washed with PBS three times for 5 min each, and incubated with the mixture of two secondary antibodies (Alexa 488 and Alexa 594) in 1% BSA for 1h at RT in the dark. The cells were washed with PBS three times for 5 min each and mounted by using Vectashield hardset with DAPI (Vector Laboratories).

Confocal Microscopy and FRET

Confocal images were sequentially acquired with Zeiss Zen software on a Zeiss LSM 780 Confocal system (Carl Zeiss Inc,) with a Zeiss Observer Z1 inverted microscope and a 25 mW Argon visible laser tuned to 488 nm and a 15 mW laser tuned to 594 nm. A 40x Plan-Apochromat 1.4 NA oil immersion objective was used at various digital zoom settings. Emission signals after sequential excitation were collected, from 490 to 553 nm or from 598 to 696 nm respectively, using individual photomultipliers. For sensitized emission FRET, an additional FRET channel was collected with 488 nm excitation and 598 to 696 nm emissions. The same confocal parameters (laser intensity, detector gain) were used for all FRET samples. mCherry alone and GFP alone samples served as FRET negative controls. FRET images were analyzed with the Zeiss Zen FRET macro.

Immunoprecipitation and western blots

Jurkat and primary T cells were plated overnight in 6–well plates with complete RPMI medium at 37°C with 5% CO_2. The next day the cells were serum starved with 0.1% BSA for 2 h, pretreated with TSP1 (2 nM) for 15 min, and incubated in the presence or absence of VEGF (30 ng/ml) for 5 min. The cells were centrifuged, washed one time with cold PBS, and lysed using NP-40 buffer. The cells were kept on ice for 5 min and centrifuged at 15,000

rpm for 15 min. The cell supernatant (300 μl) of each lysate was using 5 μl of beads to pre-clear the lysate. A 20 μl volume of Dynabeads used for immunoprecipitation of each sample. Immunoprecipitation was performed using 2 μl of VEGFR2 and Src antibodies with 300 μl of lysate at 4°C overnight. The beads were washed with NP-40 lysis buffer three times and boiled with 1X SDS buffer for 5 min at 95°C. Total protein was quantified by using the BCA method. Western blot performed using Bis–Tris 4-12% gels with NuPAGE buffer at 150 V for 45 min. The gels were transferred to polyvinylidine difluoride membranes at 45 volts for 1h. The membrane was blocked with 3% BSA in tris-buffered saline with Tween 20 (TBSTw) for at least 1 h. Human anti-CD47 (B6H12), extracellular domain of CD47 (R529), VEGFR2, or SRC antibodies (1:1000) were incubated overnight in TBSTw containing 3% BSA. Membranes were washed two times with 1X TBSTw for 10 min each. Anti-rabbit or anti mouse secondary antibodies conjugated to HRP were used diluted 1:5000. Membranes were washed three-five times with TBSTw for 15 min each, and bands were detected using chemiluminescence. Protein loading was normalized using β-actin antibody or immunoblotted for total VEGFR2, human CD47 B6H12, extracellular CD47 cleavage R259, or Src antibodies as indicated.

Real-time quantitative PCR

Total RNA was prepared using whole spleen from WT and CD47 null mice or purified subsets of splenocytes using the TRIZOL method. Jurkat cells were plated on anti-CD3 (1 μg/ml) coated plates and treated with TSP1 in the presence or absence of VEGF for 3-6 h in 2% serum. cDNA was made using the Superscript III kit from Invitrogen, and real time PCR was performed using HPRT1 and B2M primers for normalization. The following primers were used: muVEGF (5’-GCGGATCAAACCTCACCAAA–3’; 5’-TTCACATCGGCTGTGCTGTAGGA-3’), muVEGFR2 (5’-TCTGTCGCCTCGGAAGGCTCC-3’; 5’-TCGTCGCTGGAGTACACGGTG-3’), huTNFα (5’-AGAAGGGTGACCGACTCAGC-3’; 5’-TCCCAAAGTAGACCTGCCCAG-3’), huCD69 (5′-CTGGTCACCCATGGAAGTGG-3’; 5′-ACTTTCCATGCTGCTGACCT-3’), huCD40 (5’-GGCAACAATCCATTCACTTGGGAGG-3’; 5’-CCAAAGGACGTGAAGCCAGTGCCA-3’), huTOLLIP (5’-TGTTCCCCAACATGGACCAGGAGGT-3’; 5’-GCAGGGAGTTGATGGCGGCA-3’), huIL10A (5’-AGGTGGTCTCCTGGGCAGCT-3’; 5’-CTGCAGGCTAGAGATGAGGGGCA-3’), huCCL3 (5’-TGTCATCTTCCTAACCAAGCGAAG-3’; 5’-AGGCACTCAGCTCCAGGTCG-3’), huIL2 (5’-CCTGCCACAATGTACAGGATGCA-3’; 5’-GGTGCACTGTTTGTGACAAGTGC-3’), muIL2 (5’-TTGGACCTCTGCGGCATGTTC-3’; 5’-CAAATGTGTTGTCAGAGCCCT-3’), muCD69 (5’-ACGCTCTTGTTCTGAAGATGCTGC-3’; 5’-TCCAATGTTCCAGTTCACCA -3’), and muVEGFR1 (5’-TGAGGAGCTTTCACCGAACTC-3’; 5’-TGGTCTCAGTCCAGGTGAACC-3’). Real time PCR was performed using SYBR Green (Thermo Scientific) on an MJ Research Opticon I instrument (Bio-Rad) with the following amplification program: 95 °C for 15 min, followed by 40 cycles of 95 °C for 15 s, 58 °C for 20 s, 72 °C for 25 s, and 72 °C for 1 min. Melting curves were performed for each product from 30 to 95 °C, reading every 0.5 °C with a 6-s dwell time. Fold change in mRNA

expression was calculated by normalizing to HPRT1 or B2M mRNA levels, which differed in WT and CD47-null samples with equal input of RNA to generate the first strand template.

Cell proliferation Assay

Cell proliferation assay was performed using CellTiter 96® AQueous Non-Radioactive Cell Proliferation Assay (MTS) according to the manufacturer's instructions (Promega). Jurkat T and JinB8 cells (5×10^4) were plated in triplicate using 96 well plates. The cells were treated either with VEGF (30 ng/ml) or TSP1 (2 nM) or in combination. In other experiments Jurkat and JinB8 cells were treated with VEGF (30 ng/ml) or VEGF blocking antibody (10 ng/ml) alone or in combination. The cells were cultured for 72 h. Signal at 0 h was subtracted from the 72 h signal to calculate net proliferation, and results are expressed as a percentage of untreated control cell proliferation.

Pan T cell, $CD4^+$ and $CD8^+$ isolation kits were used to isolate T cells from WT and CD47−/− spleen according to the manufacturer's instructions (Miltenyi Biotech). The primary cells were prestimulated with either using anti CD3 (1 μg/ml) or in combination of anti-CD3 (2 μg/ml) and anti CD28 (5 μg/ml) as indicated. Equal numbers ($\sim2.5\times10^4$) of primary WT and CD47 −/− cells were plated on uncoated 96-well plates in triplicate. Cell proliferation was assessed using the MTS assay following treatment with TSP1 (1 μg/ml), VEGF (30 ng/ml), or SU1498 (5 μg/ml) for 72 h as described above.

Cytokine ELISA Assays

Jurkat and JinB8 T cells were plated onto anti-CD28 (3 μg/ml) and anti-CD3 (1 μg/ml) coated plates and treated with VEGF blocking antibody or TSP1 in the presence or absence of VEGF for 24 h in 2% serum. Samples of the conditioned media were analyzed for secreted IL-2, TNFα and MIPα concentrations (NCI-Leidos Biomedical Research, Inc./ FNLCR). Duplicate experimental samples were analyzed in duplicate.

Immunohistochemistry

Tissue from WT or $CD47^{-/-}$ mice was harvested and paraffin embedded. Slides were deparaffinized in Histoclear (National Diagnostics) 3 times for 5 minutes and rehydrated in graded alcohol (100%, 95 % and 70%). Antigen retrieval was performed using a coplin jar filled with Target Retrieval Solution, pH 6.10 (Dako Corporation) in a microwave for 5 min at high power, 15 min at low power and cool down for 20 min. After retrieval, slides were washed in PBS twice for 5 min. Endogenous peroxidase activity was quenched by 0.3% H_2O_2 treatment (Dako Corporation). Non-specific binding was reduced using Protein Block Serum-Free (Dako Corporation) for 10 min. The slides were incubated with VEGFR2 antibody (Cell Signaling Technologies) 1:100 overnight at 4°C. Slides were then incubated with Streptavidin-biotin (Dako LSBA+ Kit, HRP). DAB (3, 3–diaminobenzidine solution, Dako Corporation) was used as chromogen for 5 min, and hematoxylin was used for counterstaining. Negative control slides omitted the primary antibody. Images were evaluated using a Nikon Eclipse E1000 microscope equipped with a microcolor camera (RGB-MS-C), A computer-assisted counting technique with a grid filter to select cells was used to quantify the immunohistochemical staining of VEGFR2 using Image J (v. 1.42q NIH).

Flow Cytometry

Jurkat and JinB8 T cells were plated on anti-CD3 (1 μg/ml) coated plates for 6 h or on anti-CD3 + anti-CD28 for 24 h, and harvested by centrifugation. For analysis of cell surface proteins, cells were stained with fluorophore-conjugated anti-CD69, anti–VEGFR1, anti-VEGFR2, anti-VEGFR3 and anti-CD47 in separate tubes for 30 min at room temperature in FACS buffer (HBSS containing 1% FBS), washed twice with same buffer and fixed in 1% paraformaldehyde. Isotype control antibodies were used to validate flow cytometric results. Flow cytometric acquisition was performed on a LSR II cytometer with FACSDiva software (BD Biosciences). Flow cytometry data were analyzed by using FlowJO software (Tree Star).

Statistical Analysis

P-values for VEGFR2 and Src phosphorylation, cell proliferation, flow cytometry, and cell migration assays were calculated using T-tests. For all real time PCR experiments two factor ANOVA with replicates was used. P-value less than 0.05 were considered significant.

Results

Association of CD47 with VEGFR2 and Src in Jurkat T cells

To investigate the potential interaction between endogenous CD47 and VEGFR2 in T cells, we first performed confocal immunofluorescence analysis using Jurkat T lymphoma cells. Endogenous CD47 (red) and VEGFR2 (green) were partially co-localized in untreated Jurkat T cells, suggesting a physical interaction (Fig. 1A). Interaction between CD47 and VEGFR2 was confirmed by co-immunoprecipitation and FRET analysis (Fig. 1B-D). TSP1 disrupts FRET between VEGFR2 and CD47 in endothelial cells (23), and a corresponding decrease in FRET efficiency was observed in Jurkat T cells treated with TSP1 but did not reach significance (Fig 1B).

To further examine this interaction WT and a CD47-deficient Jurkat T cell mutant (JinB8) were lysed using NP-40 and immunoprecipitated using a VEGFR2 antibody. CD47 was detected by western blotting using two antibodies specific for the extracellular domain of CD47 (B6H12 and R529, Fig. 1C). Both antibodies detected the 50-55 kDa N-glycosylated and >200 kDa proteoglycan isoforms of CD47 and a previously described 36 kDa proteolytic fragment of CD47 (28, 35) in the immunoprecipitates from WT Jurkat cells that were absent in the corresponding immunoprecipitates from JinB8 cells. The CD47 antibody B6H12 detected several nonspecific bands in VEGFR2 immunoprecipitates from JinB8 cells that were not detected by the CD47 antibody R529. Treatment with VEGF did not significantly alter co-immunoprecipitation of CD47 and VEGFR2, but treatment with TSP1 in the presence of VEGF selectively inhibited association of the two smaller isoforms but not the proteoglycan isoform of CD47 with VEGFR2 (Fig. 1D). This is consistent with disruption of the VEGFR2/CD47 complex by TSP1 plus VEGF in endothelial cells but suggests that the proteoglycan isoform of CD47 remains associated with VEGFR2 in T cells (23). VEGFR2 can bind directly to heparan sulfate (36), and we propose that the proteoglycan isoform of CD47 expressed by T cells binds with high affinity to VEGFR2 and

is therefore more resistant to TSP1 inhibition than VEGFR2 binding to CD47 in endothelial cells.

Reverse immunoprecipitation using CD47 antibody and detection with anti-VEGFR2 confirmed that VEGFR2 interacts with CD47 (Fig. 1E upper panels). VEGFR2 signaling in endothelial cells recruits and activates Src (37), and co-immunoprecipitation demonstrated that VEGFR2 is associated with Src in Jurkat T cells (Fig. S1A). Src was also detected in CD47 immunoprecipitates from WT but not CD47-deficient JinB8 cells, indicating that Src is a constitutive component of this membrane complex (Fig. 1E lower panels).

TSP1 inhibits VEGFR2-Y^{1175} and Src-Y^{416} phosphorylation via CD47

TSP1 binding to CD47 suppresses VEGF-induced VEGFR2 phosphorylation in endothelial cells (23). Similar results were obtained in Jurkat T cells treated with 2 nM TSP1 (Fig. 2A, C). Addition of VEGF induced VEGFR2 phosphorylation at Y^{1175} in Jurkat cells ($p \leq 0.0001$), and pre-treatment with 0.6 or 2 nM TSP1 for 15 min prevented this response to VEGF ($p \leq 0.04$ and 0.006, respectively). The data in Fig. 2A normalized to actin was confirmed by normalizing to total VEGFR2 (Fig. S1B), indicating that TSP1 specifically inhibits VEGFR2 phosphorylation rather than merely reducing VEGFR2 expression. In contrast, TSP1 did not inhibit tyrosine phosphorylation of VEGFR2 at Y^{961} (Fig. S1C). The ability of TSP1 to modulate VEGFR2 phosphorylation required CD47 because parallel experiments performed using CD47-deficient JinB8 cells showed higher basal phosphorylation of VEGFR2 and no significant effects of VEGF or TSP1 on this signal (Fig. 2C, D). Notably, levels of total VEGFR2 appeared to be higher in the JinB8 cells (Fig. 2C).

Primary $CD3^+$ T cells isolated from spleens of WT and CD47 null mice confirmed the Jurkat T cell data. VEGF induced VEGFR2 Y^{1175} phosphorylation, and TSP1 inhibited this response in WT but not in CD47 null murine T cells (Fig. 2E, F). An elevation in total VEGFR2 was also observed in the CD47 null murine T cells.

As shown in Fig. 1E, Src interacts with the CD47/VEGFR2 complex in T cells, and VEGF-VEGFR2 signaling induces Src Y^{416} phosphorylation in endothelial cells (37). Treatment with TSP1 inhibited VEGF-induced Src Y^{416} phosphorylation in primary murine T cells and Jurkat T cells (Fig. 2B, F). At a concentration of 0.2 nM, which approximates circulating TSP1 levels in plasma, TSP1 significantly inhibited VEGF-induced Src phosphorylation at Y^{416} ($p \leq 0.02$). Notably, higher concentrations of TSP1 tended to show less Src inhibition, which may result from positive effects of TSP1 signaling through other receptors ($p \leq 0.07$, Fig 2B).

A CD47-binding peptide from TSP1 inhibits VEGFR2-Y^{1175} phosphorylation

To exclude a requirement for additional TSP1 receptors in regulating VEGFR2 we examined whether a known CD47 binding peptide derived from TSP1 (7N3) is sufficient to inhibit VEGFR2 Y^{1175} phosphorylation. Treatment of Jurkat T cells with 0.2 μM 7N3 inhibited VEGF induced VEGFR2 phosphorylation, but the control peptide 604 had no effect (Fig.S1D and E), demonstrating that engaging CD47 is sufficient for this response.

CD47 is a key regulator of VEGF and VEGFR2 expression in T cells

The elevated VEGFR2 protein expression that we observed in CD47-deficient Jurkat T cells correlated with elevated VEGFR2 mRNA levels in these cells (Fig. 3A). However, flow cytometry showed only a modest increase in cell surface levels of VEGFR2 in JinB8 relative to WT Jurkat cells (Fig 3B and C), which was statistically significant. VEGFR1 was also expressed and showed no difference in surface expression between WT and JinB8 cells (Fig 3D). Surface expression of VEGFR3 was slightly elevated in JinB8 cells (Fig 3E). Because a large fraction of the VEGFR2 in endothelial cells is intracellular and recycles to the cell surface (38), we also compared flow cytometry analysis using permeabilized and non-permeabilized cells (Fig. 3F-I). Consistent with the western blots, JinB8 cells showed higher total VEGFR2 expression than WT cells.

CD47 limits VEGF and VEGFR2 expression on murine spleen and lymphocytes

To determine whether CD47 regulates VEGF and VEGFR2 expression *in vivo*, we first analyzed mRNAs isolated from WT and CD47-null mouse spleens immediately following euthanasia (Fig. 4A). VEGF and VEGFR2 mRNA levels were approximately 13 and 7-fold higher, respectively, in CD47 null spleens compared to WT spleens. In contrast, VEGFR1 mRNA was lower in CD47 null spleens relative to WT spleens. To examine the distribution of the enhanced VEGFR2 expression in the spleen, immunohistochemical analysis of wild-type and CD47-null spleens was performed. In WT spleen, aside from highlighting the vasculature (weak membrane staining), VEGFR2 was strongly expressed (membrane and cytoplasmic staining) in some of the periarteriolar lymphoid sheaths (PALS), a T-cell rich area. In addition occasional positive cells were distributed through the red pulp. In contrast, $CD47^{-/-}$ spleen exhibited a more diffuse pattern of VEGFR2-positive cells within the PALS as well as a greater number of VEGFR2-positive cells within follicles and red pulp (Fig. 4B). Quantitative analysis of tissue sections (n=6) revealed that CD47 null mouse spleens have significantly more VEGFR2 positive cells as compared to WT ($p \leq 0.0003$, Fig. 4C). Thus, CD47 regulates VEGF production and potentially the responsiveness of splenic T cells to VEGF mediated by VEGFR2.

To define which splenic cell types exhibit CD47-dependent VEGF and VEGFR2 expression, we examined mRNA levels in several purified populations isolated from WT and CD47 null spleens. Consistent with the Jurkat cell data, $CD4^+$ T cells from CD47 null mice had elevated mRNA levels for VEGF and VEGFR2 (Fig. 4D, E). Interestingly, this was not the case for purified $CD8^+$ T cells, as VEGF and VEGFR2 were expressed 13-and 8-fold less in CD47-null CD8+ T cells, respectively. $CD19^+$ B cells from CD47 null spleen also had higher VEGFR2 expression, but CD47-null $CD11b^+$ monocytes had lower VEGFR2 expression than WT monocytes (Fig. 4F). The differential regulation of VEGF by CD47 in $CD4^+$ versus $CD8^+$ cells may be c-Myc-dependent because we recently showed differences in c-Myc expression in WT versus CD47-null $CD4^+$ and $CD8^+$ T cells (39), and VEGF is a known target of c-Myc (40, 41).

TSP1 inhibits VEGF induced cell migration in Jurkat cells

We examined several functional responses of T cells to VEGF to study cross-talk between TSP1/CD47 and VEGF signaling. Preliminary experiments using 1% to 10% FBS and 5-50

ng/ml VEGF established that 1% FBS with 30 ng/ml VEGF gave optimal stimulation of Jurkat T cell migration in a modified Boyden Chamber assay. VEGF treatment caused a significant 2.5-fold increase in cell migration as compared to a control using 1% BSA in the lower chamber ($p < 0.01$). TSP1 added to the upper chamber at 1 or 2 nM significantly inhibited VEGF induced cell migration induced by VEGF ($p \leq 0.007$ and ≤ 0.006, respectively, Fig. 5A).

VEGF inhibits T cell proliferation via VEGFR2

Proliferation of Jurkat cells in RPMI medium containing 2% FBS was assessed at 72 h. VEGF treatment inhibited proliferation of WT but stimulated proliferation of CD47-deficient cells (Fig. 5B). Both activities of VEGF were blocked by a VEGF function-blocking antibody. Therefore, CD47 is necessary for VEGF to inhibit T cell proliferation, but VEGF can also stimulate T cell proliferation via a CD47-independent mechanism. To confirm this result in primary T cells, proliferation of $CD4^+$ T cells isolated from WT and CD47-null mice was assessed in the presence of 10% FBS. The CD47-null T cells proliferated significantly more than WT $CD4^+$ T cells at 6 days ($p \leq 0.001$, Fig. 5C). Because CD47-null $CD4^+$ T cells express more VEGFR2, we tested its function in regulating proliferation using the VEGFR2 kinase inhibitor SU1498. We observed a significant decrease in CD47-null cell proliferation ($p \leq 0.00001$), whereas WT $CD4^+$ T cells at day 6 showed only marginal inhibition ($p \geq 0.08$, Fig. 5D). Therefore, autocrine production of VEGF can stimulate $CD4^+$ T cell proliferation in a VEGFR2-dependent but CD47-independent manner.

To further confirm that inhibitory VEGFR2 signaling for proliferation is CD47-dependent, Jurkat T cells were transiently transfected with VEGFR2-mCherry (WT VEGFR2) or VEGFR2-mCherry mutated to prevent phosphorylation at residue Y^{1175} (VEGFR2-mutant), and proliferation was assessed by CSFE dilution. At days 1 and 3, proliferation of cells over-expressing WT VEGFR2 was inhibited relative to cells over-expressing the phosphorylation-deficient mutant. This occurred despite more persistent expression for the mutant VEGFR2 construct relative to that of the WT construct (Fig 6A, B). Therefore, expression of functional VEGFR2 specifically limits proliferation of T cells that express CD47.

CD47-dependent regulation of TCR signaling by TSP1 and VEGF

TSP1 signaling via CD47 inhibits TCR signaling, including induction of the early activation marker CD69 (28, 33, 42). Consistent with the previous report that VEGF inhibits T cell activation (19), VEGF treatment resulted in a 4-fold reduction in CD69 mRNA expression induced by activation of WT Jurkat T cells in the presence of anti-CD3+CD28 for 24 h (Fig. 7A). Addition of TSP1 reversed the inhibition of CD69 mRNA induction by VEGF in cells as did the VEGF blocking antibody, which increased CD69 mRNA induction 3-fold. The latter result suggested that endogenous VEGF production limits activation.

CD47 deficient JinB8 cells had substantially lower basal CD69 mRNA expression, but anti-CD3+CD28 antibodies induced an 18-fold increase in CD69 mRNA (Fig. 7A). The weaker induction of CD69 in CD47-deficient cells has been reported previously and is associated

with defective integrin activation (43, 44). In contrast to WT cells, addition of VEGF did not inhibit this induction. Addition of the VEGF blocking antibody resulted in a 2-fold decrease, suggesting that VEGF has a positive effect on T cell activation in the absence of CD47.

The differential effects of VEGF on CD69 induction in the presence and absence of CD47 were confirmed at the level of cell surface protein expression (Fig. 7B, C). VEGF inhibited both the percentage of $CD69^+$ WT Jurkat T cells induced by anti-CD3+CD28 treatment for 24 h and their mean level of CD69 expression. In contrast, CD47-deficient cells were resistant to VEGF inhibition of CD69 induction by anti-CD3+CD28 (Fig. 7C). To confirm the role for endogenous VEGF suggested by the VEGF antibody blocking data, we examined the effect of a VEGF blocking antibody on CD69 induction by anti-CD3+CD28 at 24 h. Consistent with the mRNA data in Fig. 7A, the VEGF blocking antibody neutralized the inhibitory activity of VEGF in WT cells but did not CD69 induction in CD47-deficient cells (Fig. 7D, E).

A similar differential sensitivity to VEGF inhibition was seen in the absence of CD28 costimulation. Induction of CD69 mRNA by anti-CD3 alone was partially inhibited in WT but not in CD47-deficient Jurkat T cells (Fig. S2A, B and C). Under these conditions, TSP1 did not significantly reverse the inhibition by VEGF. Cell surface CD69 protein induction by anti-CD3 paralleled the mRNA changes and the results obtained with CD28 costimulation (Fig. S2C and D). Individually, VEGF and TSP1 inhibited anti-CD3-stimulated CD69 induction. However, combining TSP1 and VEGF yielded no inhibition, suggesting antagonism between TSP1 and VEGF consistent with that observed at the mRNA level. As expected, anti-CD3 stimulation resulted in a weaker induction of CD69 protein expression in CD47-deficient cells, and VEGF and TSP1 alone or in combination did not inhibit this induction. Therefore, the presence of CD47 plays a positive role in T cell activation as reported previously and presumably mediated by integrin activation (44), but the inhibitory effects of VEGF and TSP1 on T cell activation also require CD47.

A similar partial inhibition by VEGF of anti-CD3-stimulated CD69 mRNA induction was observed using WT primary murine T cells (Fig. S2E). CD47-null murine T cells were more resistant to anti-CD3 for inducing CD69 mRNA under the same conditions, but addition of VEGF in the presence of anti-CD3 increased CD69 mRNA expression (Fig. S2F), further supporting a positive effect of VEGF on activation of T cells lacking CD47.

CD47-dependent effects of VEGF on T cell activation were not limited to CD69 induction. A similar dependence on CD47 was observed for modulation by VEGF of additional activation-dependent cytokines and a chemokine. CD28 costimulation was required for induction of IL-2 in CD47-null murine T cells, so we used these conditions to compare with WT T cell responses (Fig. 7F). Anti-CD3+CD28 induced a 14-fold increase in IL-2 mRNA, and VEGF inhibited this induction to baseline levels. The VEGFR2 inhibitor SU1498 blocked inhibition by VEGF confirming that this inhibition is mediated by VEGFR2. Although TSP1 is known to inhibit IL-2 induction (43), addition of TSP1 in the presence of VEGF resulted in a 3-fold increase in IL-2 mRNA, providing further evidence of antagonism between TSP1 and VEGF to regulate T cell activation responses. Induction of IL-2 mRNA in CD47 null T cells was not inhibited by exogenous VEGF, but SU1498

reduced induction 2-fold, again consistent with endogenous VEGF being an autocrine activator in the absence of CD47. As expected, TSP1 did not alter IL-2 induction in the CD47 null cells. Thus, VEGF signaling via VEGFR2 negatively regulates IL-2 induction in primary murine T cells in a CD47-dependent manner, but autocrine production of VEGF signaling positively regulates IL-2 induction in a CD47-independent manner.

VEGF partially inhibited the induction of TNFα mRNA stimulated by anti-CD3 in Jurkat T cells (Fig. S3A). Addition of TSP1 prevented the inhibition of TNFα induction by VEGF, providing further evidence of functional antagonism between TSP1 and VEGF. TNFα was not induced above basal levels by anti-CD3 in the CD47-deficient T cell line, but VEGF added alone or in the presence of anti-CD3 increased TNFα mRNA expression. Notably, TSP1 partially inhibited the positive effect of VEGF on TNFα mRNA in the CD47-deficient cells, indicating that antagonism between TSP1 and VEGF can be CD47-independent.

Induction of the TCR-dependent chemokine IL10A, CD40 and TOLLIP (Toll interacting protein) (42) mRNAs by anti-CD3 was also inhibited by VEGF in Jurkat cells (Fig. S3B-D). Consistent with the TNFα data, addition of TSP1 in the presence and VEGF restored induction of, IL10A and TOLLIP mRNAs in WT Jurkat T cells. Anti-CD3 failed to induce the expression of CD40, IL10A and TOLLIP mRNAs in CD47-deficient cells. However, VEGF induced expression of these genes in a CD47-independent manner.

We further investigated VEGF regulation of mRNA and protein expression induced with CD28 costimulation for 24 h in WT and CD47-deficient Jurkat T cells. IL-2, TNFα, and CCL3 (MIP-1α) mRNAs were strongly induced in WT cells under these conditions, and co-incubation with VEGF in each case significantly inhibited induction (Fig. 8A, C, E). Specificity was confirmed by reversal of the VEGF inhibition by a VEGF blocking antibody. ELISA assays for TNFα and IL-2 secretion at 24 h showed parallel VEGF inhibition of activation induced secretion and reversal by the VEGF blocking antibody. Although induction of CCL3 mRNA expression was inhibited by VEGF, no significant inhibition of CCL3 protein induction by VEGF was observed.

The CD47-deficient JinB8 T cells showed less induction of TNFα mRNA than in WT, but TNFα protein secretions was strongly induced and the mRNA and protein responses were not altered by VEGF (Fig. 8A, B). IL-2 induction was confirmed at the mRNA and protein levels and was similarly resistant to VEGF inhibition (Fig. 8C, D). CCL3 (MIP-1α) showed a moderate induction of its mRNA and strong induction of CCL3 protein secretion that was similarly resistant to VEGF inhibition (Fig. 8E, F). Therefore, CD47 is necessary for VEGF to inhibit T cell activation assessed by several methods in both human Jurkat and murine primary T cells.

Discussion

This study demonstrates that the co-localization and functional cross-talk between VEGFR2 and CD47 that was first identified in endothelial cells (23) also occurs in human and murine T cells. VEGF and the CD47 ligand TSP1 individually inhibit TCR signaling, but CD47-dependent cross talk between TSP1 and VEGF can override some of these direct inhibitory

signals to result in increased activation responses (Fig. S4). This cross-talk between CD47 and VEGFR2 has functional consequences in the regulation of T cell migration and proliferation and controls the induction of TCR activation-dependent receptors, cytokines and chemokines including CD69, IL-2, CCL3, and TNFα. We also found that expression of VEGF and VEGFR2 by $CD4^+$ T cells is limited by inhibitory CD47 signaling, and CD47 thereby controls an autocrine feedback loop in T cells involving VEGF and VEGFR2. In WT cells that express CD47 this feedback by VEGF is inhibitory. However, in human Jurkat and murine $CD4^+$ T cells lacking CD47 most inhibitory effects of VEGFR2 signaling are lost, and VEGF becomes a positive regulator of proliferation and some TCR signaling responses including the induction of IL-2. TSP1, which is known to be produced in a regulated fashion by T cells (45, 46), further modulates VEGF signaling by its interactions with CD47.

We describe a novel role of TSP1 and its receptor CD47 in VEGF signaling in T cells that provides some insight into some of the discrepancies related to the role of VEGF as an immunomodulator (18, 19). In primary murine $CD4^+$ T cells and human Jurkat T cells, CD47 functions as a negative regulator of the VEGF-VEGFR2 pathway at the level of receptor phosphorylation and downstream phosphorylation of Src. Binding of TSP1 to CD47 further inhibits VEGFR2 signaling in these cells. While TSP1 is known to modulate distinct T cell functions by engaging α4ß1 and CD47 in T cells (27), this is the first report to implicate VEGFR2 in the ability of TSP1 to modulate anti-CD3-mediated T-cell activation. The fact that CD47 differentially regulates VEGF and VEGFR2 expression in $CD4^+$ T versus $CD8^+$ T cells may also account for some conflicting published evidence regarding whether VEGF is an inhibitor or stimulator of T cell function.

CD47 signaling modulates VEGFR2 and Src phosphorylation in T cells. Treatment of CD47-expressing human Jurkat and primary murine T-cells with TSP1 inhibits VEGFR2 phosphorylation at Y^{1175} and Src at Y^{416} in a CD47-dependent manner. This is consistent with an earlier report where cross-linking CD47 on T cells using two antibodies stimulated tyrosine phosphorylation of proteins including the Src family protein tyrosine kinase p56(Lck) (47). Since CD47 does not have intrinsic tyrosine kinase activity, these downstream phosphorylation events may be secondary to perturbing the lateral association of CD47 with VEGFR2, which may prevent recruitment of Src kinases including Lck, thereby ablating the signal from VEGF binding to VEGFR2. Rapid phosphorylation of VEGFR2 at Y^{1175} mediates proliferative signals in vascular cells, but our findings support the conclusion of Ziogas et al (19) that VEGFR2 phosphorylation inhibits T cell proliferation.. We demonstrated by site-directed mutagenesis that phosphorylation of VEGFR2 at Y^{1175} is required for this anti-proliferative activity. VEGF also stimulates chemotaxis of activated T cells (43), and TSP1 signaling via CD47 inhibits VEGF-stimulated T cells migration, as we previously reported for migration of vascular cells from muscle explants stimulated by VEGF or its signaling mediator nitric oxide (48) .

We further demonstrate that CD47 signaling negatively regulates T-cell expression of VEGF and VEGFR2. Thus, CD47-deficient murine B cells and $CD4^+$ T cells but not monocytes and $CD8^+$ T cells exhibit elevated expression of VEGF and VEGFR2. Expression of VEGF by T-cells antagonizes TCR signaling and thus inhibits T-cell activation in a CD47-

dependent manner as demonstrated by the expression of the TCR activation marker CD69 and several cytokines. Recent findings also revealed that VEGF expression and VEGFR2 activation suppresses the host immune response by inhibiting CD3-mediated activation of T-cells, thereby protecting tumor cells (19). In addition to the autocrine role of VEGF, CD47 null T and B cells may stimulate angiogenesis by releasing VEGF. These data may also provide insights for understanding the recruitment and regulation of tumor associated/infiltrating lymphocytes by TSP1 in the tumor microenvironment.

Current clinical anti-angiogenic therapy employs the VEGF antibody bevacizumab to inhibit VEGF binding to VEGFR2 or VEGFR2 kinase inhibitors to block its signaling. In addition to the expected inhibition of tumor angiogenesis, blocking VEGF signaling is known to cause side effects including hypertension and thrombosis (22). The data presented here and by others demonstrates that VEGFR2 antagonists can also modulate T cell immunity in the tumor microenvironment and that T cell proliferation, migration, and activation are directly modulated by VEGF. Thus, we predict that bevacizumab and VEGFR2 inhibitory drugs can also act as enhancers of anti-tumor T cell immunity. Based on our finding that disrupting the cross-talk between CD47 with VEGFR2 increases the ability of T cells to proliferate and be activated in response to TCR stimulation, we propose that therapeutic targeting of CD47 on T cells could enhance anti-tumor T cell immunity.

Supplementary Material

Refer to Web version on PubMed Central for supplementary material.

Acknowledgments

We thank Dr. Silvio Gutkind for providing SU1498 and Dr. Laura Maile for the R529 antibody.

Abbreviations used in this article

FRET	fluorescence resonance energy transfer
MTS	[3-(4,5-dimethylthiazol-2-yl)-5-(3-carboxymethoxyphenyl)-2-(4-sulfophenyl)-2H-tetrazolium, inner salt
TSP1	thrombospondin-1
VEGF	vascular endothelial growth factor-A
VEGF BK Ab	VEGF blocking antibody
VEGFR	VEGF receptor

References

1. Carmeliet P, Ferreira V, Breier G, Pollefeyt S, Kieckens L, Gertsenstein M, Fahrig M, Vandenhoeck A, Harpal K, Eberhardt C, Declercq C, Pawling J, Moons L, Collen D, Risau W, Nagy A. Abnormal blood vessel development and lethality in embryos lacking a single VEGF allele. Nature. 1996; 380:435–439. [PubMed: 8602241]

2. Dvorak HF. Vascular permeability factor/vascular endothelial growth factor: a critical cytokine in tumor angiogenesis and a potential target for diagnosis and therapy. J Clin Oncol. 2002; 20:4368–4380. [PubMed: 12409337]
3. Ptaszynska MM, Pendrak ML, Bandle RW, Stracke ML, Roberts DD. Positive feedback between vascular endothelial growth factor-A and autotaxin in ovarian cancer cells. Mol Cancer Res. 2008; 6:352–363. [PubMed: 18337445]
4. Samuel S, Fan F, Dang LH, Xia L, Gaur P, Ellis LM. Intracrine vascular endothelial growth factor signaling in survival and chemoresistance of human colorectal cancer cells. Oncogene. 2011; 30:1205–1212. [PubMed: 21057529]
5. Cao Y, E G, Wang E, Pal K, Dutta SK, Bar-Sagi D, Mukhopadhyay D. VEGF exerts an angiogenesis-independent function in cancer cells to promote their malignant progression. Cancer Res. 2012; 72:3912–3918. [PubMed: 22693250]
6. Hamerlik P, Lathia JD, Rasmussen R, Wu Q, Bartkova J, Lee M, Moudry P, Bartek J Jr. Fischer W, Lukas J, Rich JN, Bartek J. Autocrine VEGF-VEGFR2-Neuropilin-1 signaling promotes glioma stem-like cell viability and tumor growth. J Exp Med. 2012; 209:507–520. [PubMed: 22393126]
7. Lee J, Ku T, Yu H, Chong K, Ryu SW, Choi K, Choi C. Blockade of VEGF-A suppresses tumor growth via inhibition of autocrine signaling through FAK and AKT. Cancer Lett. 2012; 318:221–225. [PubMed: 22182449]
8. Lee J, Yu H, Choi K, Choi C. Differential dependency of human cancer cells on vascular endothelial growth factor-mediated autocrine growth and survival. Cancer Lett. 2011; 309:145–150. [PubMed: 21683519]
9. Byrne AT, Ross L, Holash J, Nakanishi M, Hu L, Hofmann JI, Yancopoulos GD, Jaffe RB. Vascular endothelial growth factor-trap decreases tumor burden, inhibits ascites, and causes dramatic vascular remodeling in an ovarian cancer model. Clin Cancer Res. 2003; 9:5721–5728. [PubMed: 14654557]
10. Casanovas O. Cancer: Limitations of therapies exposed. Nature. 2012; 484:44–46. [PubMed: 22481354]
11. Ferrara N. The role of VEGF in the regulation of physiological and pathological angiogenesis. EXS. 2005:209–231. [PubMed: 15617481]
12. Bergers G, Benjamin LE. Tumorigenesis and the angiogenic switch. Nat Rev Cancer. 2003; 3:401–410. [PubMed: 12778130]
13. Gabrilovich DI, Chen HL, Girgis KR, Cunningham HT, Meny GM, Nadaf S, Kavanaugh D, Carbone DP. Production of vascular endothelial growth factor by human tumors inhibits the functional maturation of dendritic cells. Nat Med. 1996; 2:1096–1103. [PubMed: 8837607]
14. Oyama T, Ran S, Ishida T, Nadaf S, Kerr L, Carbone DP, Gabrilovich DI. Vascular endothelial growth factor affects dendritic cell maturation through the inhibition of nuclear factor-kappa B activation in hemopoietic progenitor cells. J Immunol. 1998; 160:1224–1232. [PubMed: 9570538]
15. Gabrilovich D, Ishida T, Oyama T, Ran S, Kravtsov V, Nadaf S, Carbone DP. Vascular endothelial growth factor inhibits the development of dendritic cells and dramatically affects the differentiation of multiple hematopoietic lineages in vivo. Blood. 1998; 92:4150–4166. [PubMed: 9834220]
16. Gabrilovich DI, Ishida T, Nadaf S, Ohm JE, Carbone DP. Antibodies to vascular endothelial growth factor enhance the efficacy of cancer immunotherapy by improving endogenous dendritic cell function. Clin Cancer Res. 1999; 5:2963–2970. [PubMed: 10537366]
17. Kusmartsev S, Gabrilovich DI. Immature myeloid cells and cancer-associated immune suppression. Cancer Immunol Immunother. 2002; 51:293–298. [PubMed: 12111117]
18. Basu A, Hoerning A, Datta D, Edelbauer M, Stack MP, Calzadilla K, Pal S, Briscoe DM. Cutting edge: Vascular endothelial growth factor-mediated signaling in human CD45RO+ CD4+ T cells promotes Akt and ERK activation and costimulates IFN-gamma production. J Immunol. 2010; 184:545–549. [PubMed: 20008289]
19. Ziogas AC, Gavalas NG, Tsiatas M, Tsitsilonis O, Politi E, Terpos E, Rodolakis A, Vlahos G, Thomakos N, Haidopoulos D, Antsaklis A, Dimopoulos MA, Bamias A. VEGF directly suppresses activation of T cells from ovarian cancer patients and healthy individuals via VEGF receptor Type 2. Int J Cancer. 2012; 130:857–864. [PubMed: 21445972]

20. Mor F, Quintana FJ, Cohen IR. Angiogenesis-inflammation cross-talk: vascular endothelial growth factor is secreted by activated T cells and induces Th1 polarization. J Immunol. 2004; 172:4618–4623. [PubMed: 15034080]
21. Roberts DD, Miller TW, Rogers NM, Yao M, Isenberg JS. The matricellular protein thrombospondin-1 globally regulates cardiovascular function and responses to stress via CD47. Matrix Biol. 2012; 31:162–169. [PubMed: 22266027]
22. Isenberg JS, Martin-Manso G, Maxhimer JB, Roberts DD. Regulation of nitric oxide signalling by thrombospondin 1: implications for anti-angiogenic therapies. Nat Rev Cancer. 2009; 9:182–194. [PubMed: 19194382]
23. Kaur S, Martin-Manso G, Pendrak ML, Garfield SH, Isenberg JS, Roberts DD. Thrombospondin-1 inhibits VEGF receptor-2 signaling by disrupting its association with CD47. J Biol Chem. 2010; 285:38923–38932. [PubMed: 20923780]
24. Vallejo AN, Mugge LO, Klimiuk PA, Weyand CM, Goronzy JJ. Central role of thrombospondin-1 in the activation and clonal expansion of inflammatory T cells. J Immunol. 2000; 164:2947–2954. [PubMed: 10706681]
25. Reinhold MI, Lindberg FP, Kersh GJ, Allen PM, Brown EJ. Costimulation of T cell activation by integrin-associated protein (CD47) is an adhesion-dependent, CD28-independent signaling pathway. J Exp Med. 1997; 185:1–11. [PubMed: 8996237]
26. Li Z, He L, Wilson K, Roberts D. Thrombospondin-1 inhibits TCR-mediated T lymphocyte early activation. J Immunol. 2001; 166:2427–2436. [PubMed: 11160302]
27. Li Z, Calzada MJ, Sipes JM, Cashel JA, Krutzsch HC, Annis DS, Mosher DF, Roberts DD. Interactions of thrombospondins with alpha4beta1 integrin and CD47 differentially modulate T cell behavior. J Cell Biol. 2002; 157:509–519. [PubMed: 11980922]
28. Kaur S, Kuznetsova SA, Pendrak ML, Sipes JM, Romeo MJ, Li Z, Zhang L, Roberts DD. Heparan sulfate modification of the transmembrane receptor CD47 is necessary for inhibition of T cell receptor signaling by thrombospondin-1. J Biol Chem. 2011; 286:14991–15002. [PubMed: 21343308]
29. Miller TW, Kaur S, Ivins-O'Keefe K, Roberts DD. Thrombospondin-1 is a CD47-dependent endogenous inhibitor of hydrogen sulfide signaling in T cell activation. Matrix Biol. 2013; 32:316–324. [PubMed: 23499828]
30. Lamy L, Foussat A, Brown EJ, Bornstein P, Ticchioni M, Bernard A. Interactions between CD47 and thrombospondin reduce inflammation. J Immunol. 2007; 178:5930–5939. [PubMed: 17442977]
31. Grimbert P, Bouguermouh S, Baba N, Nakajima T, Allakhverdi Z, Braun D, Saito H, Rubio M, Delespesse G, Sarfati M. Thrombospondin/CD47 interaction: a pathway to generate regulatory T cells from human CD4+ CD25- T cells in response to inflammation. J Immunol. 2006; 177:3534–3541. [PubMed: 16951312]
32. Manna PP, Frazier WA. The mechanism of CD47-dependent killing of T cells: heterotrimeric Gi-dependent inhibition of protein kinase A. J Immunol. 2003; 170:3544–3553. [PubMed: 12646616]
33. Barazi HO, Li Z, Cashel JA, Krutzsch HC, Annis DS, Mosher DF, Roberts DD. Regulation of integrin function by CD47 ligands. Differential effects on alpha vbeta 3 and alpha 4beta1 integrin-mediated adhesion. J Biol Chem. 2002; 277:42859–42866. [PubMed: 12218055]
34. Roberts DD CJ, Guo N. Purification of thrombospondin from human platelets. Journal of tissue culture methods. 1994; 16:217–222.
35. Maile LA, Allen LB, Veluvolu U, Capps BE, Busby WH, Rowland M, Clemmons DR. Identification of compounds that inhibit IGF-I signaling in hyperglycemia. Exp Diabetes Res. 2009; 2009:267107. [PubMed: 20111736]
36. Xu D, Fuster MM, Lawrence R, Esko JD. Heparan sulfate regulates VEGF165- and VEGF121-mediated vascular hyperpermeability. J Biol Chem. 2011; 286:737–745. [PubMed: 20974861]
37. Sun Z, Li X, Massena S, Kutschera S, Padhan N, Gualandi L, Sundvold-Gjerstad V, Gustafsson K, Choy WW, Zang G, Quach M, Jansson L, Phillipson M, Abid MR, Spurkland A, Claesson-Welsh L. VEGFR2 induces c-Src signaling and vascular permeability in vivo via the adaptor protein TSAd. J Exp Med. 2012; 209:1363–1377. [PubMed: 22689825]

38. Gampel A, Moss L, Jones MC, Brunton V, Norman JC, Mellor H. VEGF regulates the mobilization of VEGFR2/KDR from an intracellular endothelial storage compartment. Blood. 2006; 108:2624–2631. [PubMed: 16638931]
39. Kaur S, Soto-Pantoja DR, Stein EV, Liu C, Elkahloun AG, Pendrak ML, Nicolae A, Singh SP, Nie Z, Levens D, Isenberg JS, Roberts DD. Thrombospondin-1 signaling through CD47 inhibits self-renewal by regulating c-Myc and other stem cell transcription factors. Sci Rep. 2013; 3:1673. [PubMed: 23591719]
40. Kang J, Rychahou PG, Ishola TA, Mourot JM, Evers BM, Chung DH. N-myc is a novel regulator of PI3K-mediated VEGF expression in neuroblastoma. Oncogene. 2008; 27:3999–4007. [PubMed: 18278068]
41. Hu YH, Kong SQ, Kong HB, Wu JL, Chen Z. Targeting c-Myc on cell growth and vascular endothelial growth factor expression in IN500 glioblastoma cells. Chin Med J (Engl). 2012; 125:2025–2031. [PubMed: 22884072]
42. Lerner CG, Horton MR, Schwartz RH, Powell JD. Distinct requirements for C-C chemokine and IL-2 production by naive, previously activated, and anergic T cells. J Immunol. 2000; 164:3996–4002. [PubMed: 10754290]
43. Shin JY, Yoon IH, Kim JS, Kim B, Park CG. Vascular endothelial growth factor-induced chemotaxis and IL-10 from T cells. Cell Immunol. 2009; 256:72–78. [PubMed: 19249018]
44. Reinhold MI, Green JM, Lindberg FP, Ticchioni M, Brown EJ. Cell spreading distinguishes the mechanism of augmentation of T cell activation by integrin-associated protein/CD47 and CD28. Int Immunol. 1999; 11:707–718. [PubMed: 10330276]
45. Futagami Y, Sugita S, Vega J, Ishida K, Takase H, Maruyama K, Aburatani H, Mochizuki M. Role of thrombospondin-1 in T cell response to ocular pigment epithelial cells. J Immunol. 2007; 178:6994–7005. [PubMed: 17513749]
46. Li SS, Liu Z, Uzunel M, Sundqvist KG. Endogenous thrombospondin-1 is a cell-surface ligand for regulation of integrin-dependent T-lymphocyte adhesion. Blood. 2006; 108:3112–3120. [PubMed: 16835379]
47. Ticchioni M, Deckert M, Mary F, Bernard G, Brown EJ, Bernard A. Integrin-associated protein (CD47) is a comitogenic molecule on CD3-activated human T cells. J Immunol. 1997; 158:677–684. [PubMed: 8992983]
48. Isenberg JS, Ridnour LA, Dimitry J, Frazier WA, Wink DA, Roberts DD. CD47 is necessary for inhibition of nitric oxide-stimulated vascular cell responses by thrombospondin-1. J Biol Chem. 2006; 281:26069–26080. [PubMed: 16835222]

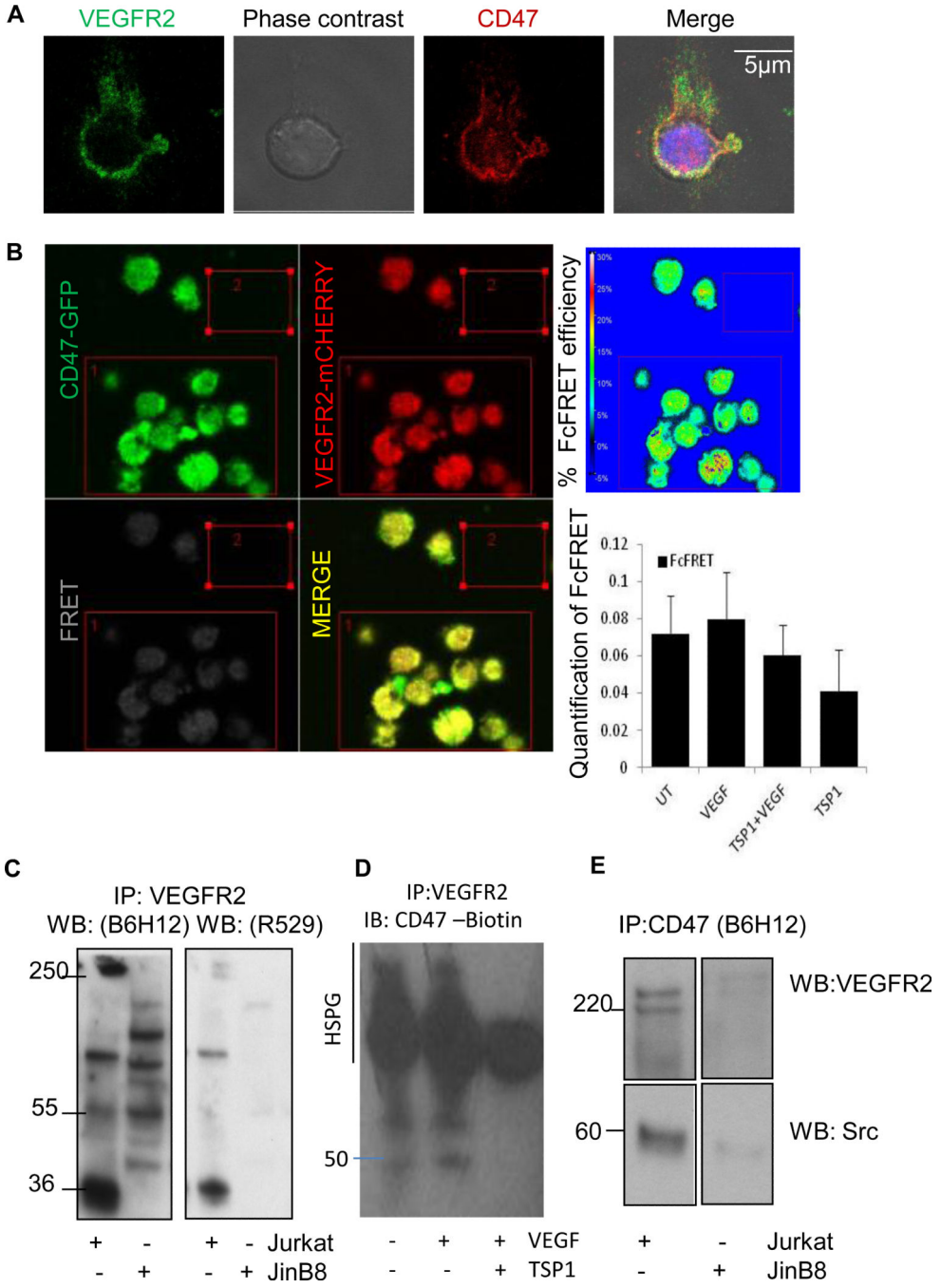

Figure 1.

CD47 and VEGFR2 co-localize in Jurkat T Cells. **(A).** Confocal microscopy of Jurkat cells attached to poly-L-lysine-coated slides. Cells were fixed and stained for CD47 (red) and VEGFR2 (green). **(B).** FRET analysis by re-expression of CD47-GFP (green) and expression of VEGFR2-mCHERRY (red) in JinB8 cells. Images are representative for untreated cells. Graph presents mean % ± SD Fc-FRET for untreated cells and cells pretreated with TSP1 (2 nM) on ice for 20 min followed by incubation in the presence or absence of VEGF (30 ng/ml) for 10 min at 37°C. **(C)** VEGFR2 immunoprecipitation from

lysates of Jurkat and CD47-deficient JinB8 cells. Proteins were separated by SDS-PAGE and detected by western blotting using CD47 antibodies specific for the intact protein (B6H12; left panel) or the CD47 extracellular domain (R529; right panel). **(D).** Immunoprecipitation of cell lysates from Jurkat cells using VEGFR2 antibody and western blot was performed with biotin-labeled anti-human CD47 Antibody. **(E).** Immunoprecipitation of cell lysates from Jurkat and JinB8 cells using CD47 antibody B6H12. Western blots were probed with VEGFR2 (Top Panels) or c-Src antibody (Bottom Panels). Numbers indicate the migration positions of protein markers in kDa.

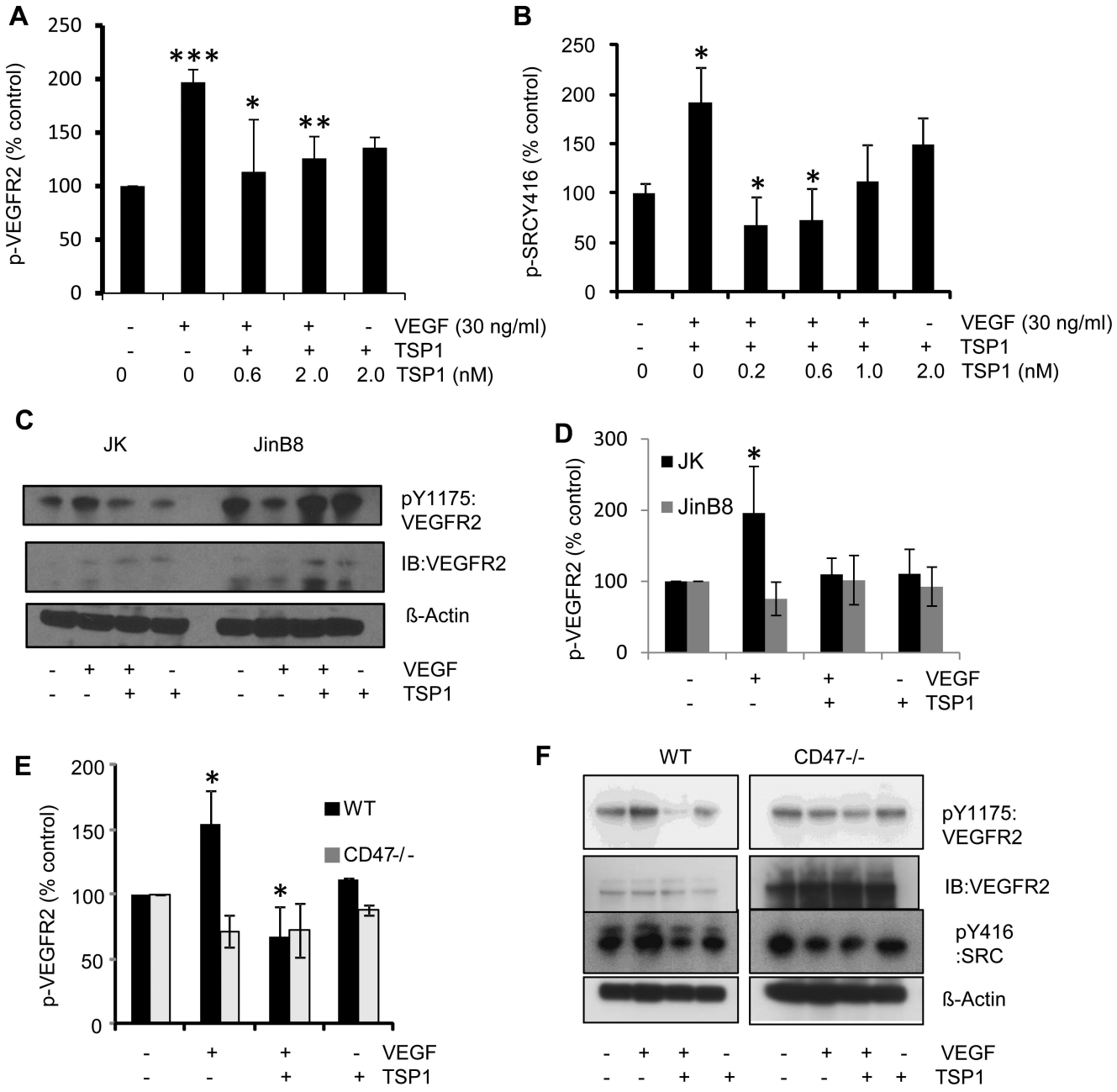

Figure 2.

TSP1 inhibits VEGFR2-Y^{1175} and Src-Y^{416} phosphorylation in Jurkat T cells *via* CD47. **(A).** VEGFR2-Y^{1175} phosphorylation in Jurkat T cells. Cells were treated with TSP1 at the indicated doses (nM) in the presence or absence of VEGF (30 ng/ml). Cell lysates were assayed by Western blotting for phosphorylation of tyrosine-1175 of VEGFR2. Results were quantified by densitometry scans, normalized to actin, and are the average of at least 3 experiments. Pairwise p-values for the following data sets: UT vs; VEGF (0.0001), UT vs TSP1 (2 nM) (0.002), TSP1 (0.6 nM) +VEGF (0.04), TSP1 (2 nM) +VEGF (0.006) respectively. **(B).** Src-Y^{416} phosphorylation in Jurkat T cells. Cells were treated and assayed as in (A). Pairwise P values are as follows: UT vs; VEGF (0.02), TSP1 (2 nM) (0.5), TSP1

(1 nM) +VEGF (0.05), TSP1 (0.6 nM) +VEGF, (0.002), TSP1 (0.2 nM) +VEGF, (0.02), respectively. **(C).** VEGFR2-Y^{1175} phosphorylation in Jurkat (WT) and JinB8 (CD47-deficient) T cells. Cells were treated with TSP1 (2 nM) in the presence or absence of VEGF (30 ng/ml), and cell lysates were assayed for phosphorylation of tyrosine-1175 of VEGFR2 by western blotting. **(D).** Quantification of the extent of VEGFR2 phosphorylation in (C) was determined by densitometry and is the average of 3 different experiments. Pairwise P values are as follows: Jurkat UT vs VEGF (0.02); VEGF vs TSP1+VEGF, (0.02); UT vs TSP1 (0.3); JinB8 UT vs VEGF (0.12) and VEGF vs TSP1+VEGF (0.19); UT vs TSP1 (0.32). **(E).** TSP1 inhibits VEGFR2 phosphorylation in primary T cells *via* CD47. $CD3^+$ T cells were isolated from the spleens of WT and CD47-null mice. Cells were cultured on anti-CD3 coated plates for 2-3 days and then treated with TSP1 (2 nM) in the presence or absence of VEGF (30 ng/ml). Cell lysates were assayed for VEGFR2-Y^{1175} phosphorylation as in (A). **(F).** Quantification of Western blot in (E) as determined by densitometry and is the average of three independent experiments. Pairwise P values for WT: UT vs VEGF (0.02), UT vs TSP1+VEGF (0.07), VEGF vs TSP1+VEGF (0.01) and UT vs TSP1 (0.005). P values for $CD47^{-/-}$: UT vs VEGF (0.05), UT vs TSP1 (0.03), UT vs TSP1+VEGF (0.14) and VEGF vs TSP1+VEGF (0.8). For western blot quantification a two sample t-test assuming equal variance was performed, and a P- Value less than 0.05 is used as significant (*).

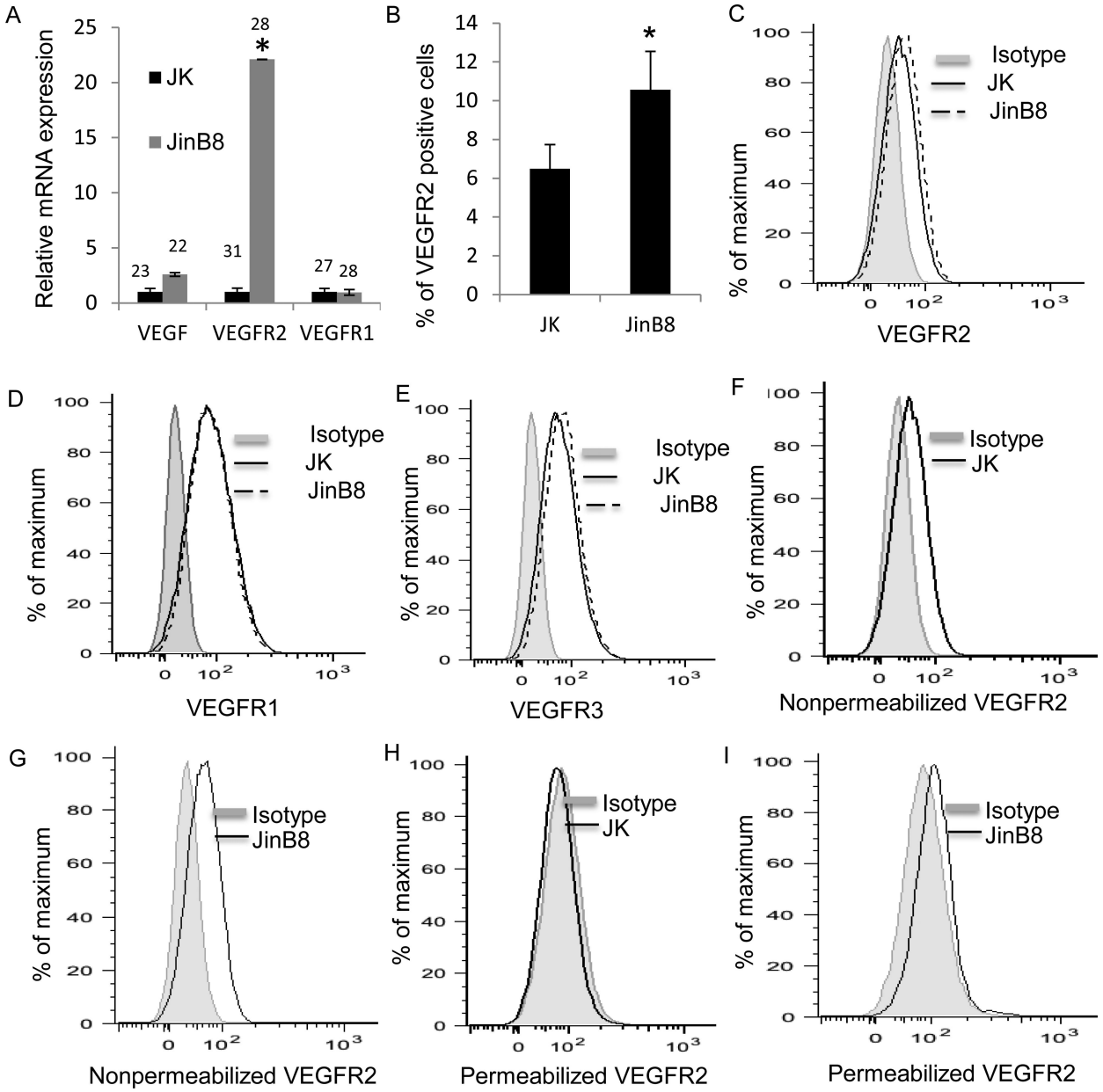

Figure 3.

CD47 signaling inhibits VEGF and VEGF receptor expression. **(A).** Relative mRNA levels of the indicated genes in Jurkat and JinB8 T cells. Results are the average of at least three independent experiments and were analyzed using a two-sample t-test assuming equal variance. **(B).** VEGFR2 protein expression in Jurkat and JinB8 cells. **(C-E).** Protein expression levels for the indicated genes in WT Jurkat and CD47-deficient JinB8 T cells. A two sample t-test assuming equal variance was used for statistical analysis. P-values less than 0.05 were considered significant (*). **(F-I).** VEGFR2 levels in non-permeabilized and permeabilized Jurkat T and JinB8 cells. Representative plots are shown, and replicate experiments for those presented in F and G did not show significant differences.

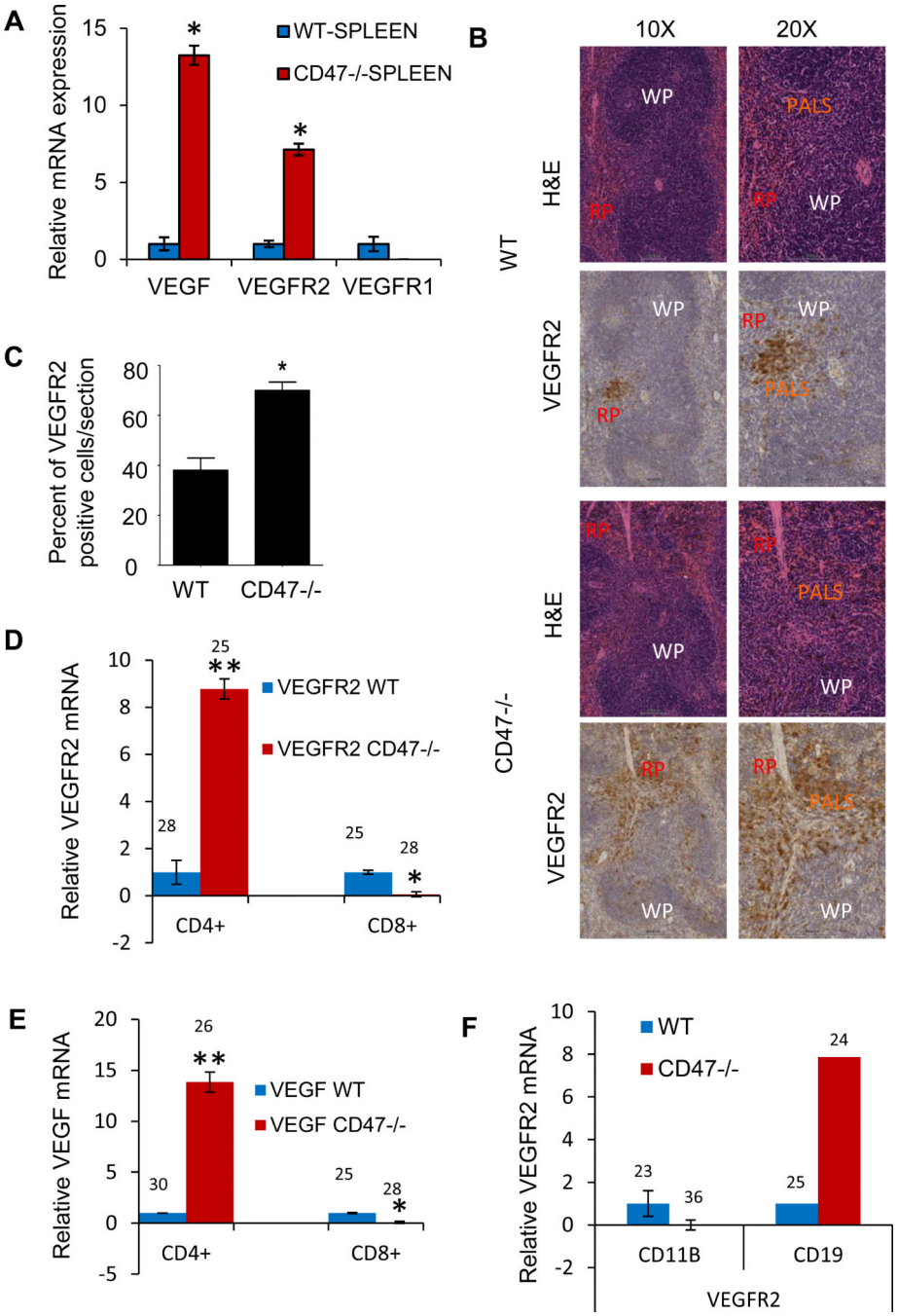

Figure 4.

VEGF and VEGF receptor expression in spleen and splenic cells from WT and CD47$^{-/-}$ mice. **(A)** Relative mRNA levels for the indicated genes using RNA isolated from WT and CD47$^{-/-}$ mouse spleens normalized to HPRT1 controls (Ct = 29 and 34 in WT and CD47−/− spleen tissues, respectively). **(B).** Immunohistochemical staining of spleens from WT and CD47$^{-/-}$ mice using an anti-VEGFR2 antibody. **(C).** Quantification of VEGFR2-positive regions from (A). **(D, E).** Relative mRNA levels of VEGF and VEGFR2 in CD4^{+} and CD8^{+} primary T cells isolated from WT and CD47$^{-/-}$ mouse spleens. Mean raw Ct values are

indicated. **(F)** Relative mRNA levels of VEGF and VEGFR2 in $CD11b^+$ and $CD19^+$ primary cells isolated from WT and CD47 null mouse spleens. Mean raw Ct values are indicated. Two-way ANOVA with replicates was used for analysis. And a P-value less than 0.05 is used as significant (*).

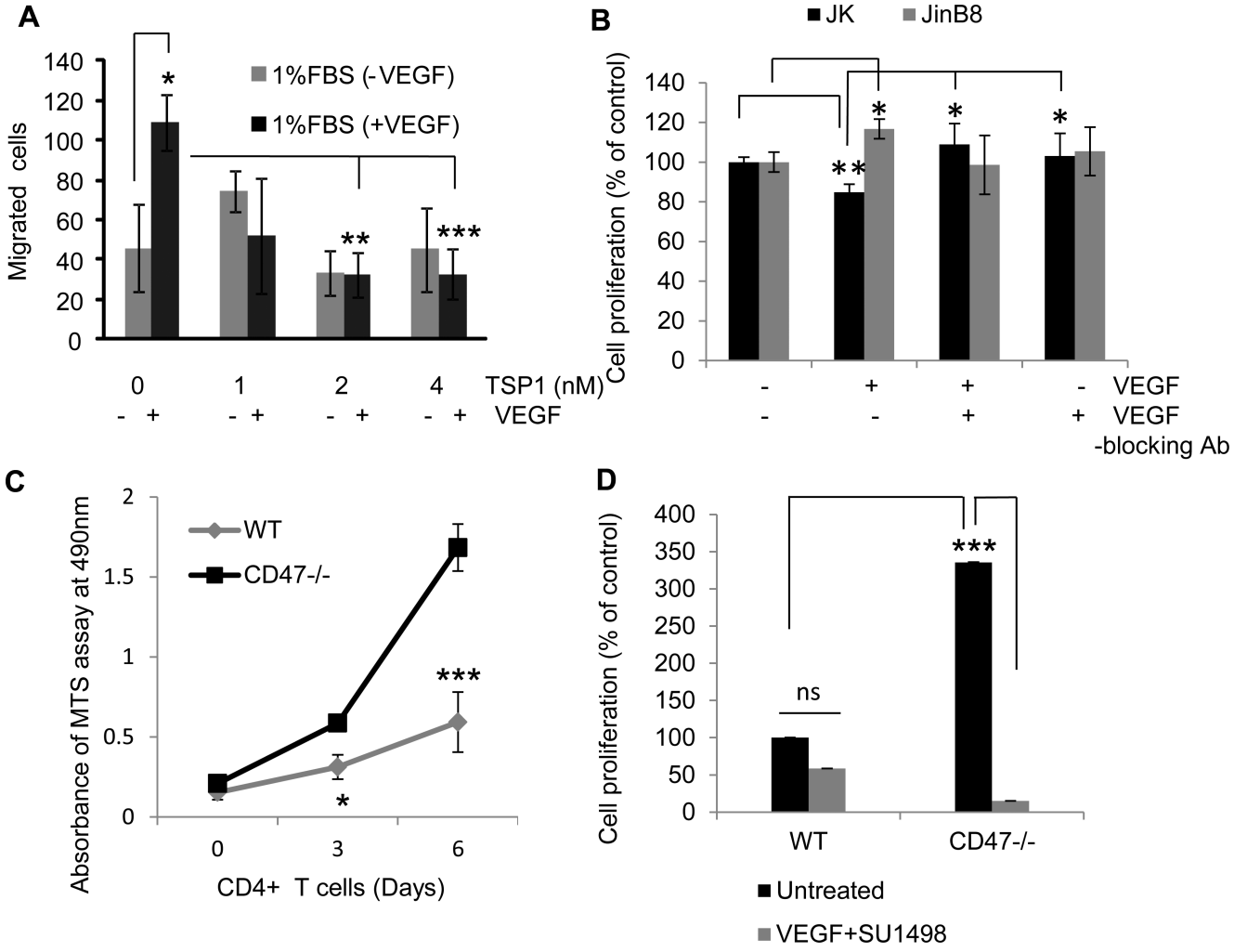

Figure 5.

CD47 mediates cross-talk between TSP1 and VEGF to modulate T cell migration and proliferation. **(A).** TSP1 inhibits VEGF-induced chemotaxis. Jurkat cells were serum-starved for 2 h and added to the upper compartment of a Boyden chamber apparatus. A gelatin-coated membrane (pore size 3 μm) separated the lower chamber to which 1% FBS with or without VEGF (30 ng/ml) was added. TSP1 at the indicated doses was added to the top chamber. Migration was allowed to proceed for 3 h, and the cells were fixed and counted in three fields using a 20X objective. A two sample t-test assuming equal variances was used, and P-values are as follows: UT vs VEGF 0.01; VEGF vs TSP1(2 nM) and VEGF 0.007; VEGF vs TSP1(4 nM)+VEGF 0.006. **(B).** Jurkat and JinB8 cells were treated with VEGF in the presence or absence of VEGF blocking antibody. VEGF inhibited cell proliferation in Jurkat T cells but not in cells lacking CD47. Jurkat and JinB8 cells were plated in 96-well plates in triplicate in the presence or absence of VEGF (30 ng/ml) or TSP1 (4 nM) as indicated. Cell proliferation was measured after 72 h using an MTS assay. The time zero background values were subtracted from the 72 h readings, and net proliferation is presented as a percentage of the untreated control. **(C).** Proliferation on anti-CD3 of $CD4^+$ T cells isolated from spleens of C57BL/6 (WT) and $CD47^{-/-}$ mice. Values for the MTS

proliferation assay were calculated as in (B). **(D).** Proliferation was as assayed in (C) except cells were incubated with and without the VEGFR2 inhibitor SU1498, and a two sample t-test assuming equal variances was used for statistical analysis.

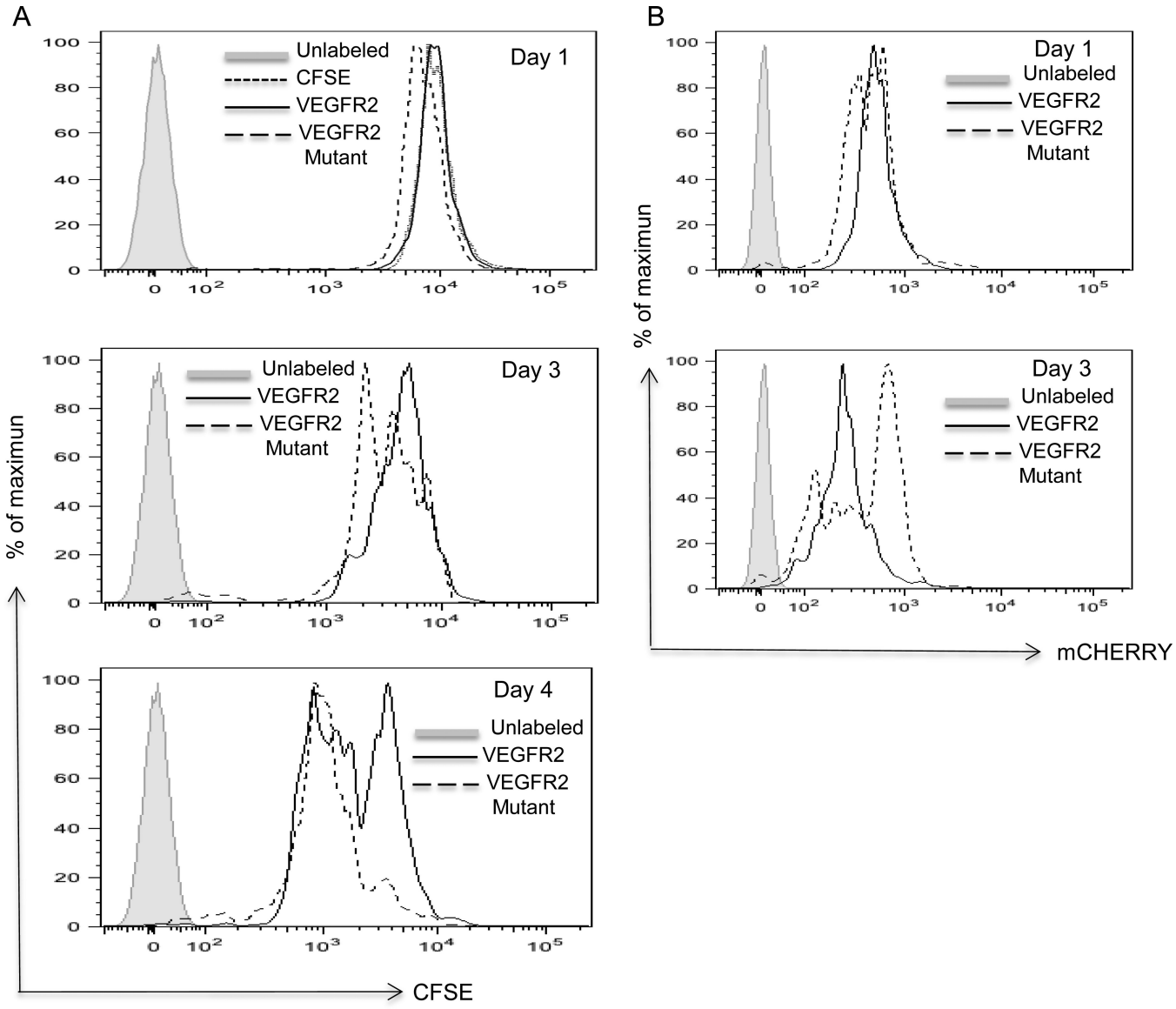

Figure 6.

VEGFR2-Y^{1175} is necessary for inhibiting T cell proliferation. VEGFR2-mCherry or the $Y^{1175}F$ mutant VEGFR2-mCherry plasmids were transfected into Jurkat T cells. **(A)**. Cell proliferation was measured using CSFE by flow at the indicated times after transfection. **(B)**. Preferential retention of VEGFR2 $Y^{1175}F$-mCherry mutant expression in transfected Jurkat cells.

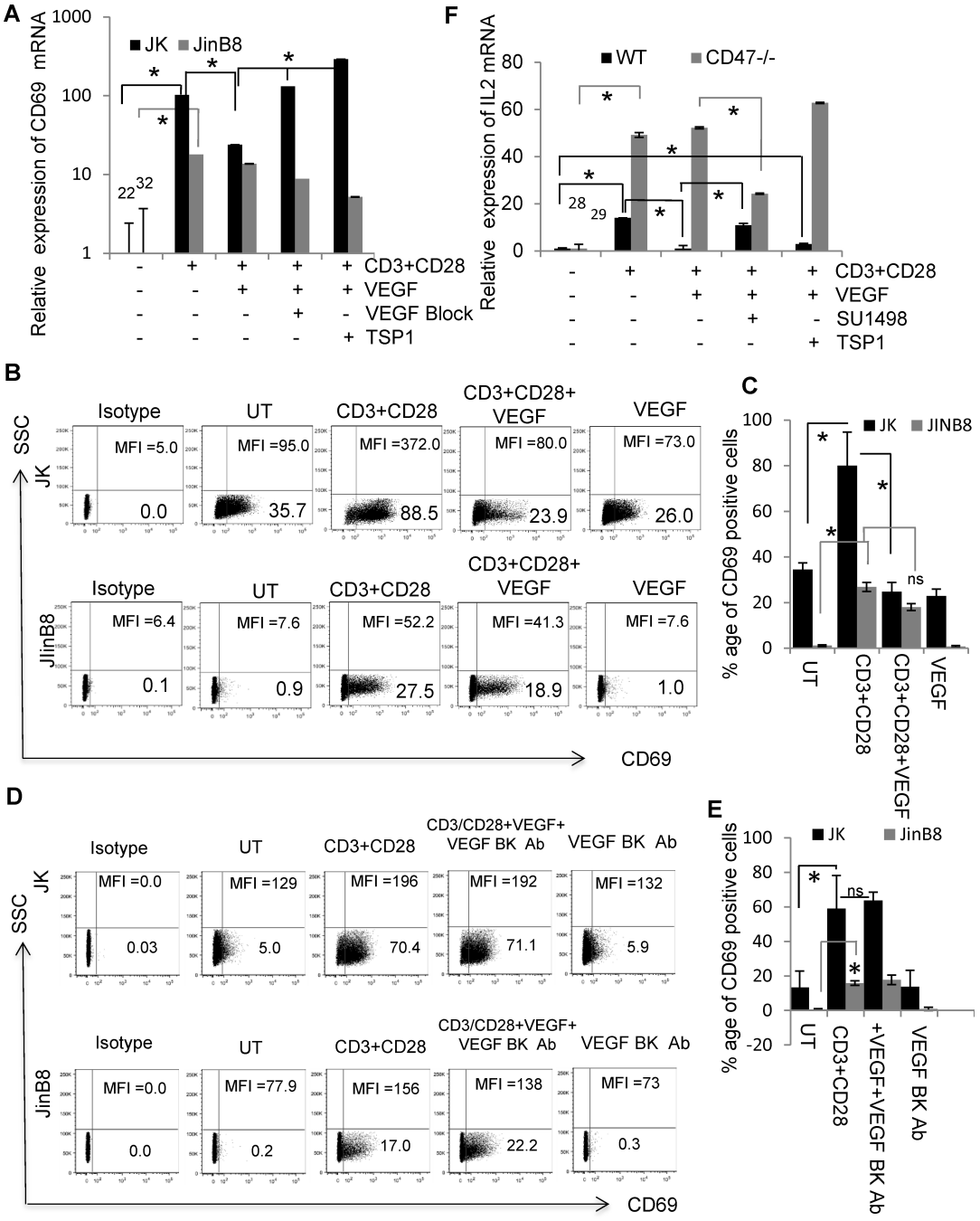

Figure 7.

TSP1 and VEGF synergize to inhibit early TCR marker expression only in CD47-positive cells. **(A).** CD69 mRNA levels in WT (A) or CD47-deficient Jurkat T cells incubated on anti-CD3 and CD28 antibody-coated plates in the presence or absence of VEGF, VEGF blocking antibody and TSP1as indicated. **(B).** CD69 cell surface expression on WT or CD47-deficient Jurkat T cells plated on anti-CD3 and anti-CD28 antibody-coated plates in the presence or absence of VEGF for 24 h. **(C).** Quantification of CD69 positive cells using flow cytomery analysis (n=3) A two sample t-test assuming equal variances was used for

statistical analysis. **(D).** CD69 cell surface expression on WT or CD47-deficient Jurkat T cells plated on anti-CD3 and anti-CD28 antibodies-coated plates in the presence or absence of VEGF and VEGF blocking antibody for 24 h. **(E).** Quantification of CD69 positive cells using flow cytomery analysis (n=3). Two sample t-test assuming equal variances was used for statistical analysis. **(F)** Differential regulation of IL-2 induction by VEGF and TSP1 in murine WT and CD47-null CD4+ T cells. CD4+ T cells from WT or CD47-null mice were pre-stimulated with anti-CD3 (1 μg/ml) and then incubated on immobilized anti-CD3 (2 μg/ml) + anti-CD28 (5 μg/ml) for 24 h in the absence or presence of 30 ng/ml VEGF, 5 μg/ml SU1498, or 2 nM TSP1 as indicated. IL-2 mRNA expression is expressed relative to that in the respective untreated T cells. For statistical analysis, two factor ANOVA with replication was used, and P-values less than 0.05 were considered significant (*).

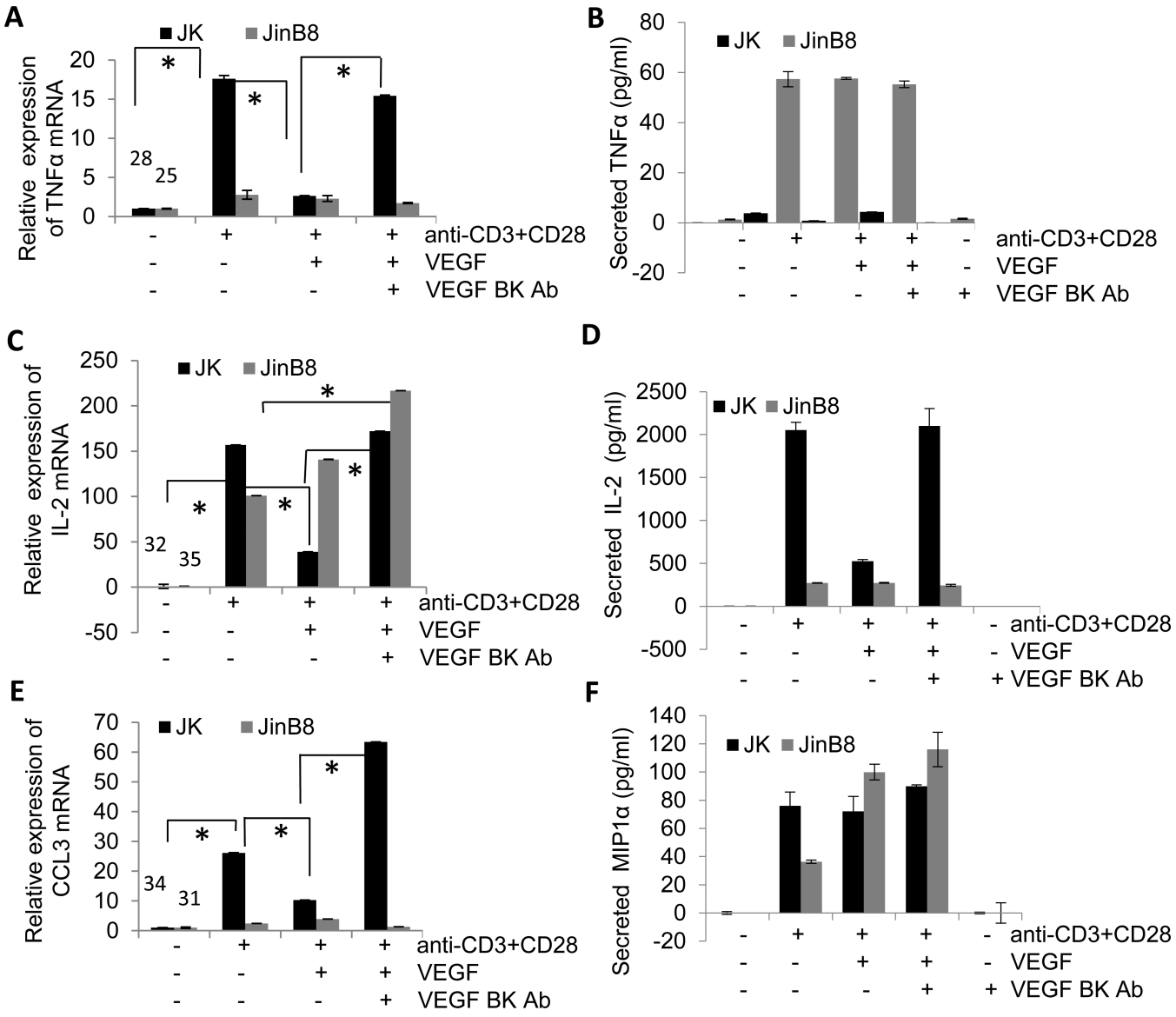

Figure 8.

Differential regulation of mRNA and protein expression of TNF, IL-2 and CCL3 induction by VEGF in Jurkat and JinB8 T cells. (A, C and E) Jurkat and JinB8 cells were incubated on immobilized anti-CD3 (1 μg/ml) + anti-CD28 (3 μg/ml) antibodies for 24 h in the absence or presence of 30 ng/ml VEGF and VEGF blocking antibody as indicated, and mRNA levels were assessed using real time PCR. Results were analyzed using two factor ANOVA with replication, and P-values less than 0.05 were considered significant (*). (B, D and F) Jurkat and JinB8 cells were immobilized on anti-CD3+CD28 coated plates and treated with VEGF blocking antibody in the absence or presence of VEGF for 24 h. The supernatant was collected and cell ELISAs were performed.